

## Fractal approach to lightning radiation on a tortuous channel

G. Vecchi, D. Labate, and F. Canavero

Dipartimento di Elettronica, Politecnico, Torino, Italy

**Abstract.** In this paper the radiation from a geometrically fractal (i.e., arbitrarily irregular) discharge channel is investigated from the point of view of engineering applications of fractal geometry. Numerical results are presented for lightning return stroke radiation, which demonstrate that the time waveform of radiated field (in the Fraunhofer region) is a fractal, and within the framework of employed approximations, it has the same fractal dimension as the channel path. Some implications of this finding are discussed along with the limitations of the model.

### 1. Introduction and Motivations

The gross structure of the electromagnetic field generated by lightning has received considerable attention up to now, being the major responsible of the lightning-related hazards to systems (e.g., see the comprehensive review of *Gardner* [1990a], and the classical book by *Uman* [1987]). Much less attempt of modeling has insofar received the fine structure of the field radiated by lightning discharges, whose time history however exhibits a jagged shape with remarkable spectral content in several bands of practical importance for communication, control, and generally consumer electronics. In addition, the VHF and UHF portions of the radiated field are presently regarded as the clues to the (insofar little understood) initiation region of the lightning [see *Gardner*, 1990a, preface]. Likewise, beside mechanical and thermal problems, electrostatic discharges (ESD) generate broad-spectrum electromagnetic fields (up to the gigahertz range) that interfere with proper operation of most types of electronic units, especially those hosted aboard satellites [*Paul*, 1992, chap. 12; *Borleitner*, 1989, chap. 5]. Hence a model capa-

ble of describing discharge-radiated field would be of importance, for example, for use in simulators of control or communication systems.

The fine-structure, higher-frequency noise due to discharges is most likely due to microscopical physical mechanisms of chaotic or almost-chaotic nature, whose microscopical description is very difficult. Therefore a macroscopical, or phenomenological, model that bypasses the analysis at the microscopical level, would be of importance for practical simulation purposes.

At this macroscopical level, fractals should be appropriate descriptors, since fractal geometry is the natural framework for the description of chaos [*Barnsley*, 1988, chap. 4]. Much like the moments of a statistical distribution that have a physical meaning and allow a good description of a stationary noise by any process sharing the same statistical characterization, fractals are characterized by some parameters that are intimately related to the physics of the phenomena. Therefore fractals with the same parameters as those observed in experiments or measured discharges will give a good description of the fine structure of discharge-generated transient fields. The main interest in engineering application of fractals is the observation that very complicated shapes can be described in a simple way by using fractals. More precisely, a complex shape can be

Copyright 1994 by the American Geophysical Union.

Paper number 93RS03030.  
0048-6604/94/93RS-03030\$08.00

described by a few parameters of a fractal object (e.g., an iterative generation algorithm), so that a complex shape can be represented, for a given degree of accuracy, with a small quantity of information.

**Fractals in the description of discharge paths.** Fractal description techniques have been successfully applied to the geometrical description of the discharges, that is, for the description of the discharge paths [see *Femia et al.*, 1993]. Confirming the intuitive expectation that the ragged, irregularly looking discharge paths will be fractals, this research showed the usefulness of the fractal description and proved the fractality hypothesis for the treelike shapes of discharge phenomena. The results have been obtained for interelectrode discharges, but there is no reason against their application to lightning.

**Fractals in the description of complex physical data.** Besides the widely known use of fractals to computer generate real-looking pictures [*Mandelbrot*, 1982], it has recently been shown that fractal techniques can be employed to represent (that is, approximate) real complex patterns [*Barnsley*, 1988, chap. 5]. In addition to that, the parameters of the fractal approximation of measured data contain information strictly tied to the physics of the phenomenon, as it has been shown for gas combustion [*Strahle*, 1991].

**Aim of this work.** On the basis of the above considerations, one can suppose that fractals can be used to obtain good phenomenological models of the macroscopical quantities of interest.

This idea works in two directions. On the one side, the problem is that of tying together a fractal description of the discharge and a fractal description of the discharge-generated field. Once this is done, one can attempt to go in a reversed direction, using the so-obtained information to construct a phenomenological model of the discharge from observed data.

In this paper we address the problem of finding the field radiated by a fractal-modeled discharge, and of analyzing such a field from the

fractal point of view, in order to assess the fractality of the temporal field and seek the relationship between the fractal parameters of the model of the discharge and those of the field.

Because of the availability of reference data, in this paper we have restricted ourselves to lightning. As a representative of different physical mechanisms of discharge that may result in fractal objects, we have considered the example of a tortuous channel described by a fractal path. The effect of channel tortuosity on the return stroke radiation was investigated by *LeVine and Meneghini* [1978a], using a double-exponential current pulse form. It was then already known that channel tortuosity resulted in a jagged transient response that appeared very similar to typically measured field waveforms, and that increasing tortuosity could eventually obliterate the standard smooth waveform of the radiated field. Based on this data, we attempt a fractal-based description of the effect of channel tortuosity.

The problem can thus be stated as that of finding the transient field radiated by a pulse traveling along a fractal channel and subsequently analyze the relationship between the fractality of the path and of the transient field waveform. Although fractal electrodynamics has been investigated by several researchers in the past years (e.g., see the recent review of *Jaggard* [1990]), the authors are not aware of any other work addressing this problem.

The work presented in this paper is slanted toward the engineering applications of fractals. Therefore no claim of mathematical rigor or completeness is made upon the tools and conclusions of this work.

## 2. Transient Radiation from a Fractal Current Path

### 2.1. Radiation from a tortuous channel

The lightning channel is considered composed of  $N$  straight segments and is assumed lossless. In the relevant literature [see *Nucci et al.*,

1990], channel losses are accounted for heuristically by a frequency-independent attenuation length. This correction does not appear in previous works dealing with path geometry [LeVine and Meneghini, 1978a; Gardner, 1990b], and in order to compare our results with the existing ones we have not included losses in our analysis. However, a discussion on this approximation can be found in section 3.3. Radiation is calculated without taking into account the possible lumped admittances at junctions between segments ("kinks"), so that the total field is the sum of the elemental fields radiated by each current segment. The ground is assumed flat and perfectly conducting; therefore the derivation of the radiated field is carried out in free space, the addition of the image contribution being straightforward. In particular, at ground level the vertical component of the electric field will be twice as much its free-space counterpart. Corrections due to lossy ground can be inserted as detailed by Gardner [1990b], but these, as well as the effect of ionosphere, do not appear to appreciably change the structure of the transient field. The above-listed approximations appear to yield a field response in good agreement with measured results [LeVine and Meneghini, 1978a]. Although the results are the same as given by LeVine and Meneghini [1978a, b], we will briefly summarize them and the methods used, in order to point out the simplicity deriving from the use of the Green's function for the fields.

In view of the considerations above, the task reduces to that of evaluating ( $N$  times) the electromagnetic fields produced by a straight, arbitrarily oriented channel along which propagates a traveling wave current. This problem admits to a closed-form solution in both frequency and time domains only if the current pulse propagates at a velocity  $v = c$  ( $c$  being the speed of light) [Fang and Wenbing, 1989]. A closed-form solution in time domain is important to reduce computation times, control the errors inherent to discretization, and grant insight into the radiation mechanisms. Therefore, in the practically

important case  $v \neq c$ , we will use the Fraunhofer (far field) approximation, that allows the desired closed form solution.

We consider thus a straight segment with center located at  $\mathbf{r}'_i$  and extending for a length  $L_i$  along the direction  $\hat{\mathbf{s}}_i$ , carrying a current  $I(\ell, \omega)$ , where  $\ell \in [-L_i/2, L_i/2]$  is the rectilinear coordinate along the segment. We want to find the radiated electric field  $\mathbf{E}_i(\mathbf{r})$  at the observer location  $\mathbf{r}$  and denote  $\mathbf{r}_i = \mathbf{r} - \mathbf{r}'_i$ . Accepting a phase error bounded by  $\delta\pi$  ( $\delta$  being a specified tolerance), and provided that  $r_i/L_i > (L_i/4\lambda)(1/\delta)$  over the frequency band of interest, on use of the free-space dyadic Green's function for the electric field [Tai, 1971; Felsen and Marcuvitz, 1973, Section 1.1b], after straightforward manipulations one can write the radiated electric field  $\mathbf{E}_i(\mathbf{r}, \omega)$  as

$$\begin{aligned} \mathbf{E}_i(\mathbf{r}, \omega) = & -j\omega\mu \frac{e^{-jk r_i}}{4\pi r_i} \times \\ & \times [A_i K_{r_i} \hat{\mathbf{r}} + B_i (K_{\theta_i} \hat{\boldsymbol{\theta}} + K_{\phi_i} \hat{\boldsymbol{\phi}})] \times \\ & \times \int_{-L_i/2}^{L_i/2} I(\ell, \omega) e^{jk a_i \ell} d\ell, \end{aligned} \quad (1)$$

where the hat denotes a unit vector, and

$$A_i = \frac{2j}{k r_i} + \frac{2}{k^2 r_i^2}, \quad B_i = 1 - \frac{j}{k r_i} - \frac{1}{k^2 r_i^2}, \quad k = \omega/c,$$

$$K_{r_i} = a_i = \hat{\mathbf{r}} \cdot \hat{\mathbf{s}}_i, \quad K_{\theta_i} = \hat{\boldsymbol{\theta}} \cdot \hat{\mathbf{s}}_i, \quad K_{\phi_i} = \hat{\boldsymbol{\phi}} \cdot \hat{\mathbf{s}}_i.$$

The current on the channel is assumed to be a pulse traveling along with velocity  $v$  regardless of channel kinks:

$$i(s, t) = i_0(t - s/v), \quad I(s, \omega) = I_0(\omega) e^{-j\omega s/v},$$

$s$  being the total arc length along the (piecewise linear) channel path. Summing up all contributions from the  $N$  segments, one gets the total radiated field,

$$\begin{aligned} E_r(\mathbf{r}, \omega) = & 2Z_0 I_0(\omega) \times \\ & \times \sum_{i=1}^N C_{r,i} \frac{1}{4\pi r_i} e^{-j\omega(r_i/c + s_i/v)} \times \\ & \times Q(r_i, \omega) \left( e^{j\omega\tau_i/2} - e^{-j\omega\tau_i/2} \right) \end{aligned} \quad (2)$$

$$E_{\alpha}(\mathbf{r}, \omega) = -Z_0 I_0(\omega) \times \sum_{i=1}^N C_{\alpha,i} \frac{1}{4\pi r_i} e^{-j\omega(r_i/c + s_i/v)} \times (1 + Q(r_i, \omega)) \left( e^{j\omega\tau_i/2} - e^{-j\omega\tau_i/2} \right), \quad (3)$$

where  $\alpha$  indicates either  $\theta$  or  $\phi$ ,  $Z_0 = \sqrt{\mu_0/\epsilon_0}$ ,  $C_{\alpha,i} = K_{\alpha,i}/(c/v - a_i)$  and

$$\tau_i = (1 - a_i v/c) L_i/v, \quad s_i = \sum_{n=1}^{i-1} L_n + \frac{L_i}{2},$$

$$Q(r, \omega) = \frac{c/r}{j\omega} + \frac{(c/r)^2}{(j\omega)^2}. \quad (4)$$

The time domain counterpart of (2) is obtained directly via Fourier inversion. Letting

$$t_i^{(1)} = r_i/c + s_i/v - \tau_i/2, \quad t_i^{(2)} = t_i^{(1)} + \tau_i, \quad (5)$$

the  $E_{\theta}$  and  $E_{\phi}$  components read

$$E_{\alpha}(\mathbf{r}, t) = \frac{Z_0}{4\pi r} \times \sum_{i=1}^N C_{\alpha,i} \left\{ \left[ i_0(t - t_i^{(1)}) - i_0(t - t_i^{(2)}) \right] + \left[ i_1(t - t_i^{(1)}) - i_1(t - t_i^{(2)}) \right] + \left[ i_2(t - t_i^{(1)}) - i_2(t - t_i^{(2)}) \right] \right\} \quad (6)$$

with

$$i_1(t) = \frac{c}{r} \int_0^t i_0(t') dt', \quad i_2 = \frac{c}{r} \int_0^t i_1(t') dt', \quad (7)$$

while  $E_r$  is obtained from (6) on substituting  $-2C_{r,i}$  for  $C_{\alpha,i}$  and deleting the term in  $i_0$ . By inspection of (1), one notes that if  $r_i \gg \lambda$  over the entire band of interest, the terms in (7) may be neglected. By geometric considerations, one sees that each term in the sums in (6) appears as contributions originating from the lower and upper ends of each segment. Last, note that, although  $v$  has been assumed constant, it may be let to have different values on different segments.

**Pulse shape.** The current waveform assumed in this simulation is the standard model

proposed by *Uman* [1987] and modified by *LeVine and Meneghini* [1978b]:

$$I_0(t) = I_a [e^{-\alpha t} - e^{-\beta t}] + I_b [e^{-\gamma t} - e^{-\delta t}]$$

with the following parameters:

$$\alpha = 2 \times 10^4 \text{s}^{-1}, \quad \beta = 2 \times 10^5 \text{s}^{-1}, \quad \gamma = 10^3 \text{s}^{-1}$$

$$\delta = 2 \times 10^4 \text{s}^{-1}, \quad I_a = 30 \text{kA}, \quad I_b = 2.5 \text{kA}.$$

## 2.2. Fractal Channel

**Fractal dimension.** The most important parameter of a fractal object is its fractal dimension  $D$  [*Barnsley*, 1988, chap. 5; *Mandelbrot*, 1982, chap. I], which is a (quantitative) measure of the “jaggedness” of a curve, or equivalently, of its space-filling property. A fractal curve has a fractal dimension  $D > 1$ , as contrasted to a standard (Euclidean) curve that has  $D = 1$ , while a two-dimensional surface (e.g., a black square) has  $D = 2$ . For “standard” (nonfractal) objects the fractal dimension coincides with the standard dimension  $E$ , called topological. Throughout this paper, the fractal dimension has been computed using both the box counting algorithm [*Barnsley*, 1988, chap. 5; *Peitgen and Saupe*, 1988, chap. 1; *Dubuc et al.*, 1989] and the variation method introduced by *Dubuc et al.* [1989], which we have extended to the evaluation of fractal dimension of nonplanar curves, as in the case of the three-dimensionally tortuous channel. The first method is standard and allows the determination of fractality scales (see later); the latter has been proven [*Dubuc et al.*, 1989] to be reliable and robust, especially when the curve is self-affine (as in the case of the field) instead of self-similar (like the channel). In this work we have employed an efficiency-improved version of the box counting algorithm due to *Strahle* [1991], and differences between the results of the *Strahle* version of the box counting and variation algorithms are negligible.

For the sake of conciseness, we give here a brief description of the basic box counting algorithm only, especially in order to set the ground for the discussion on the scales of fractality. For

a plane curve, the box counting entails properly normalizing the axes so that the curve lies within a unit square which has been subdivided in (small) boxes with side  $1/2^k$  and then counting the number  $N_b(k)$  of boxes in which there lies at least one point of the curve. The box size is then recursively halved ( $1/2^{k+1}, 1/2^{k+2}, \dots$ ), and the count is repeated. If one plots the number of occupied boxes  $N_b(m)$  versus the reciprocal of the box side, i.e.  $2^m$ , for  $m = k, k + 1, \dots$  on a doubly logarithmic graph, the points are found to lie on a straight line, whose slope is the sought-for fractal dimension. In practice, the points do not lie exactly on a straight line; hence the confidence interval in the linear approximation (e.g., see Figure 4) yields the uncertainty bound of the algorithm for the fractal dimension estimation. Both the Strahle version of the box counting and the variation algorithm result in a graph like the one described above: therefore all fractal dimensions are expressed as  $D \pm \Delta D$ , and  $\Delta D$  is the uncertainty on the dimension estimation. For nonplanar curves ( $E = 3$ ), as in the case of the three-dimensionally tortuous channel, one considers a unit cube and cubic boxes instead of squares. In all of the reported results, when we refer to the box counting dimension, we mean the Strahle version of the method.

**Fractal model of the channel and fractal dimension.** The channel is described as a function of the altitude  $z$ ; that is, letting  $\mathbf{r} = \mathbf{r}_c$  denote the points of the channel, the equation of the channel path is parametrically described by  $\mathbf{r}_c(z) = x(z)\hat{x} + y(z)\hat{y} + z\hat{z}$ , where  $x(z)$  and  $y(z)$  are two fractals curves. In order to keep closer to the probable random nature of the channel formation,  $x(z)$  and  $y(z)$  are two statistically independent fractal random processes. For the numerical generation of the channel path, we have employed here the random midpoint displacement algorithm [Peitgen and Saupe, 1988, chap. 2], that builds up the fractal iteratively, starting from a straight segment and randomly displacing the midpoint, then proceeding on each of the two halves and so on. The channel appears thus as piecewise linear. Because of the iterative halving, the seg-

ments decrease in length as  $1/2^m$  and because of the fractal nature of the process, the total length increase as  $2^{m(D_c-1)}$ , where the number  $D_c$  represents the fractal dimension of the channel [Peitgen, 1988 chap. 1].

In the midpoint displacement algorithm the variance of the independent discrete random variables used in the displacement process is a function of the fractal dimension  $D_c$  of the channel, which is the parameter to be specified. The fractals so constructed appear to simulate the so-called "fractal random walk" [Mandelbrot, 1982, chap. VIII]. In this paper we have considered explicitly the case of  $x$  and  $y$  fractal curves having the same fractal dimension, which then turns out to be the dimension of the entire (three-dimensional) channel  $D_c$ . This has been done in order to reduce the number of parameters to be considered when comparing the fractal properties of channel and field. A cursory mention to the case of different  $x$  and  $y$  fractal dimensions is made in section 3.1.

Although the fractal dimension  $D_c$  of the channel is set during the generation process, it has been evaluated using both algorithms in order to assess the intrinsic uncertainty of the dimension estimation algorithm that will be used in the analysis of the fractal properties of the field.

Being essentially concerned with return stroke, in this work, branching of the channel is not considered, because of the difficulty in modeling the return along secondary branches. In fact, the authors do not know of any work addressing this problem.

**Spatial scales of fractality.** It is apparent that while a "true" (exact) fractal is infinitely self-similar and infinitely detailed (as obtained with an infinite number of iterations), the channel generated by a finite number  $m$  of iterations is an approximate fractal, which will exhibit fractal properties only within a certain range of (spatial, in the case of the channel) scales. In particular, its fractal dimension will remain larger than its topological dimension only if observed on a scale consistently larger than the (average) length between two subsequent nodes, between which the approximate fractal is just

a straight segment. This can be seen quantitatively in Figure 4a, in which the box counting graph inflects at a threshold value, below which the fractal dimension drops to one. Such a threshold value can thus be taken as the minimum fractality scale; in fact, in the example in Figure 4a, keeping into account the normalization factor used in the box counting (6000 m, corresponding to the height of the channel), the threshold appears to approximately equal the average segment length ( $\bar{L}=90$  m).

The fact that we deal with intrinsically approximate fractals, which are such only in a limited range of scales, will clearly have an effect on the fractal properties of the radiated field.

### 3. Fractal Analysis of the Field

The field radiated from a fractal channel has been studied and discussed in the time domain and the frequency domain. Typical results are shown for the transient radiated field in Figures 1, 2 and 3 and some of the spectra are shown in Figure 5. Correctness of the results has been ensured through checks, for the case of a straight channel (not shown) and of a tortuous channel (obviously qualitative; not shown), against the simulated and measured data given by *Le Vine and Meneghini* [1978a]. In all cases, a channel with vertical ( $z$ ) extension of 6 km has been considered. The pulse velocity  $v$  is constant in Figures 1 and 2; we have used the value  $v = c/3$  which seems to (partially) account for the corona effect around the channel [*Baum and Baker*, 1990]. In Figure 3,  $v$  is constant along each straight segment but variable with height  $z$ , with  $v(z)$  exponentially decreasing from the value  $v(0) = c$  at ground level, where we suppose the initiation takes place, to the asymptotic value  $v = c/3$  with a scale height of 6000 m. This roughly simulates the variable corona along the channel [*Uman*, 1987, section 1.3; *Baum and Baker*, 1990; *Baum* 1990].

#### 3.1. Time Domain Analysis

Typical plots of the transient radiated field are reported in Figures 1, 2 and 3. Note that the

actual length of the channel considerably varies with the degree of tortuosity, here related to the fractal dimension  $D_c$ : as a result, also the flight time of the pulse along the channel, and the duration of the transient field waveform varies accordingly (see section 3.3 for a further discussion on this). In all the reported cases, the plots do not show the late part of the time response, consisting of a smooth pulse corresponding to the radiation from the top end of the channel [*Le Vine and Meneghini*, 1978b] and all fractal-based considerations apply to the jagged portion which is shown here solely (see also the considerations of section 3.3).

Fractal analysis of the transient radiated field is based on its fractal dimension  $D_f$ , that is the most important fractal parameter (see above, section 2.2).

In all of the reported cases, the field radiated by a fractal channel appears to have a fractal dimension  $D_f > 1$ , which allows to maintain that radiated field is, for a convenient time interval, a fractal itself. Moreover, within the confidence range of the employed dimension-estimating algorithms, the radiated field appears to have the same fractal dimension as the channel ( $D_f \approx D_c$ ).

Although not reported here, all of the examined cases showed the same result about fractality and fractal dimension, regardless of location in the horizontal plane ( $\phi$ ), pulse velocity ( $v$ ), fractal dimension of the channel, different and statistically independent realizations of the (random-based) channel, scale contraction of  $x$  and  $y$  (to reduce the horizontal occupation of the channel), and distance from the origin. Fields have not been computed in the near-field region, where the Fraunhofer approximation fails (in the present case the specification of an overall phase error of  $\pi/10$  sets the minimum distance at about  $r = 35$  km for the bandwidth of the input pulse). Note, however, that, closer to the source, Fraunhofer approximation fails only for the low-frequency component of the field spectrum, thus resulting in low accuracy in the late part of the transient response [*Le Vine and Meneghini*, 1978b], which is essentially smooth.

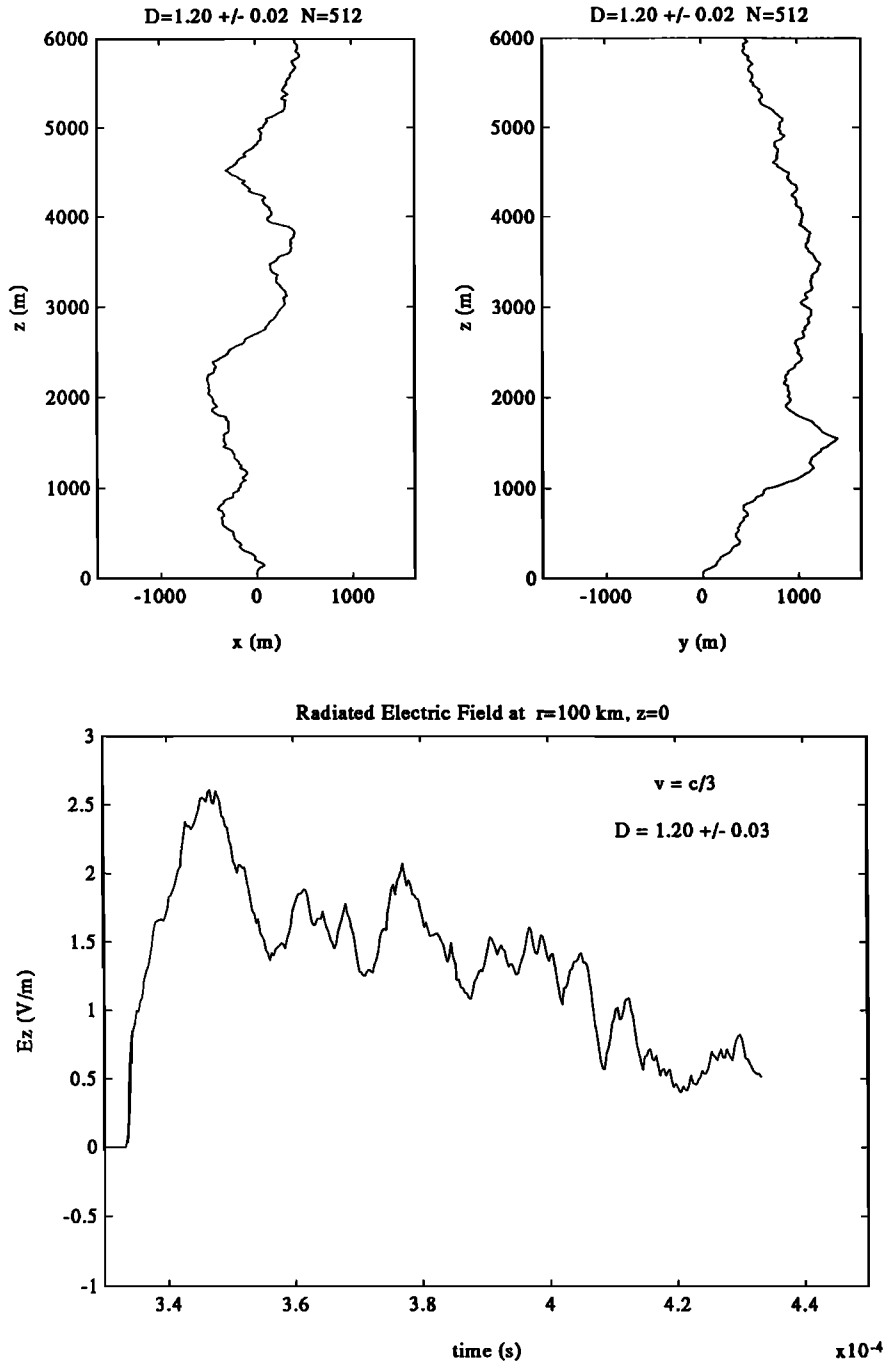


**Figure 1.** Fractality of channel and transient field. (top) The  $(x, z)$  and  $(y, z)$  projections of the channel, with fractal dimension  $D_c = 1.20 \pm 0.02$  and  $N = 512$  segments. Current pulse velocity is  $v = c/3$ . (bottom) The vertical component ( $E_z$ ) of the radiated electric field at ground level ( $z = 0$ , or  $\theta = 90^\circ$ ),  $r = 100$  km away from the channel foot, along  $\phi = 45^\circ$ . The smooth, late-time part of the waveform is not shown on the plot. The computed fractal dimension of the field is  $D_f = 1.20 \pm 0.03$ .

In this and all of the following figures the electric field is positive when directed toward the ground.

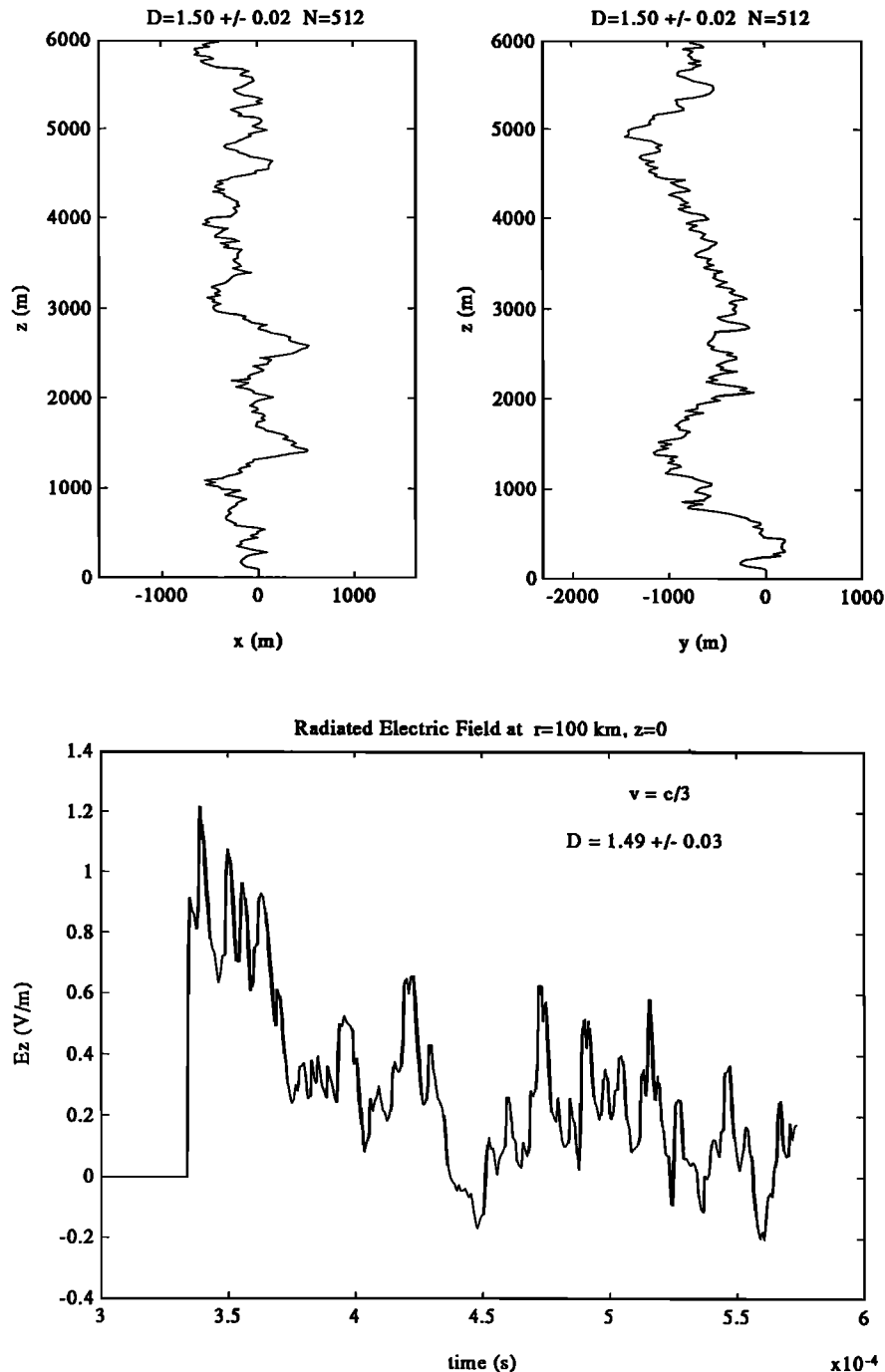


**Figure 2.** Higher fractal dimension (time domain). (top) The  $(x, z)$  and  $(y, z)$  projections of the channel, with fractal dimension  $D_c = 1.50 \pm 0.02$ . Current pulse velocity is  $v = c/3$ . (bottom) vertical component ( $E_z$ ) of the radiated electric field at ground level; horizontal location is the same as in Figure 1. Late times are not shown on the plot. The computed fractal dimension of the field is  $D_f = 1.49 \pm 0.03$ .

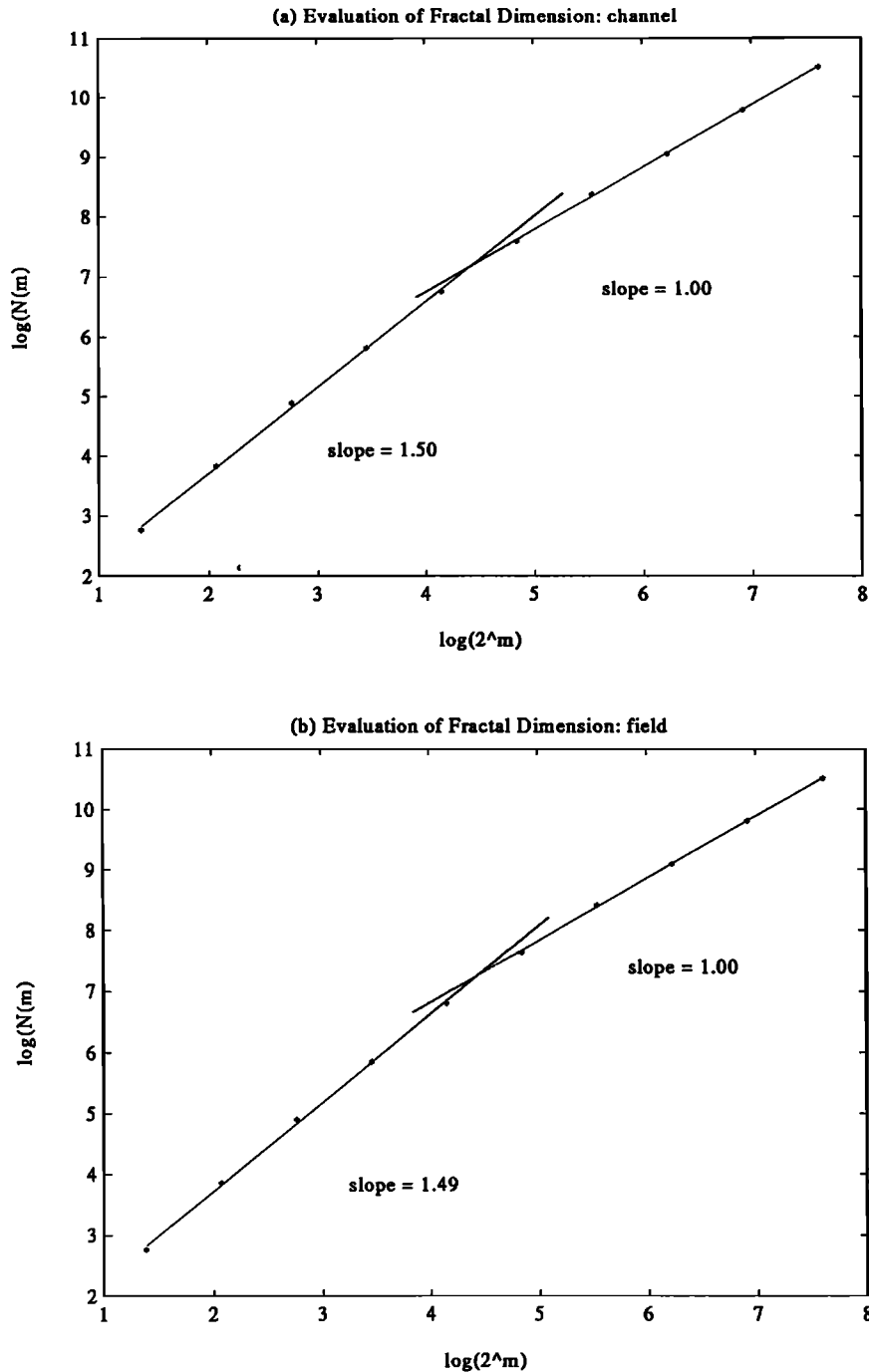


**Figure 3.** Altitude-dependent pulse velocity. Vertical component ( $E_z$ ) of the radiated electric field at ground level. Same observation location and channel ( $D_c = 1.50 \pm 0.02$ ) as in Figure 2, but pulse velocity depends on  $z$  (see text). Late times not shown on the plot. The computed fractal dimension of the field is  $D_f = 1.45 \pm 0.05$ .

Therefore fractality considerations extend below the Fraunhofer bound for distance. The results reported in this paper refer to a random-based fractal channel (see section 2); we have also tried a channel whose shape was generated through Von Koch's ("snowflake") curve [Mandelbrot, 1982, section 2.6], which is a "canonical" deterministic fractal. The results (not shown here) are the same as with the random-based fractals as far as fractality and fractal dimension are concerned. Last, the case of a (three-dimensional) channel with  $x$  and  $y$  projections having different fractal dimensions has also been examined. It appears that the radiated field has still the same fractal dimension as the channel. The value of the latter appears to lie between the values of the dimensions of the two projections, although we did not find any simple law to link the dimension of the three-dimensional path to those of its projections.

**Timescales of fractality.** As discussed above, the fractal channel is generated with a finite number of iterations, and consequently, the segment length is not vanishingly small; instead, the average segment length will have a finite value,  $\bar{L}$ . On the other hand, by inspection of equations (4), (5), and (6) one ascertains that the time lag between two subsequent arrivals is  $\tau_i$ , whose average value  $\bar{\tau}$  is approximately proportional to  $\bar{L}$ . It is clear that on a timescale smaller than  $\bar{\tau}$ , the field time waveform is smooth, and therefore  $\bar{\tau}$  sets the fractal threshold of the radiated field. This agrees with the spatial scale of fractality, seen to be  $\bar{L}$ .

In Figure 4b, the measured fractal dimension of the radiated field is shown to tend to  $D_f = 1$  (corresponding to the radiation from a straight line channel) for timescales less than  $0.9 \mu\text{s}$ , which corresponds to the value of  $\bar{\tau}$  evaluated directly as the arithmetic mean of the  $\tau_i$ . We also note that for the far field at  $z = 0$ ,  $a_i \approx 0$ , and thus (see equation (4))  $\bar{\tau} \approx \bar{L}/v$ .

### 3.2. Spectral Analysis

The fractal analysis, as discussed above in terms of the temporal shape of the waveform radiated from a fractal channel, is confirmed

from the analysis in the frequency (spectral) domain, although this latter appears less precise than its time-based counterpart, (as also noted by Dubuc [1989]). The power spectrum of the field  $S(\omega) = |E_z(\omega)|^2$ , calculated via (2) and (3), is plotted with a doubly logarithmic format in Figure 5 for the cases corresponding to Figure 1 ( $D_c = 1.20$ ) and Figure 2 ( $D_c = 1.50$ ). The power spectrum appears to be a so-called  $1/f^\beta$  spectrum; that is, there exists an asymptotic region (for large frequencies  $f$ ), whose envelope obeys a simple power law and decays as  $1/f^\beta$ ; in the following,  $\beta$  will be called spectral exponent. First of all, we note that this result is in agreement with *LeVine and Meneghini* [1978a], where the asymptotic envelope of the spectrum is found to decrease as  $1/f^4$  for a vertical straight line channel and as  $1/f^2$  for a tortuous channel.

In fact, the (randomly) tortuous channel model employed by *LeVine ad Meneghini* [1978a] appears to be a special case of the fractal random walk path employed here to describe the discharge channel, that obtains when  $D_c = 1.5$  (corresponding to normally distributed random displacements). In the general case analyzed here, the spectral exponent  $\beta$  appears to be a function of the fractal dimension  $D_c$  of the channel (which quantitatively estimates its tortuosity). The relationship that we have found agrees with *Gagnepain et al.* [1985], where the dependence of the fractal dimension  $D$  of a time series is related to the spectral exponent of its spectrum through numerical investigation. The spectral exponent  $\beta$  is found there to vary from  $\beta = 4$  for a Euclidean curve ( $D = 1$ ) to  $\beta = 1$  for a space-filling curve ( $D = 2$ ). This dependence can be explained in terms of the increase in high-frequency components of the spectrum, generated by the increased irregularity of the time series for larger values of the fractal dimension  $D$ , with reduced slope of the spectral envelope.

We can thus infer that a fractal modeling of the channel affords a good description of a broad class of tortuous discharge paths.

**Spectral scales of fractality.** The fact that the channel is a limited-scale fractal is ap-

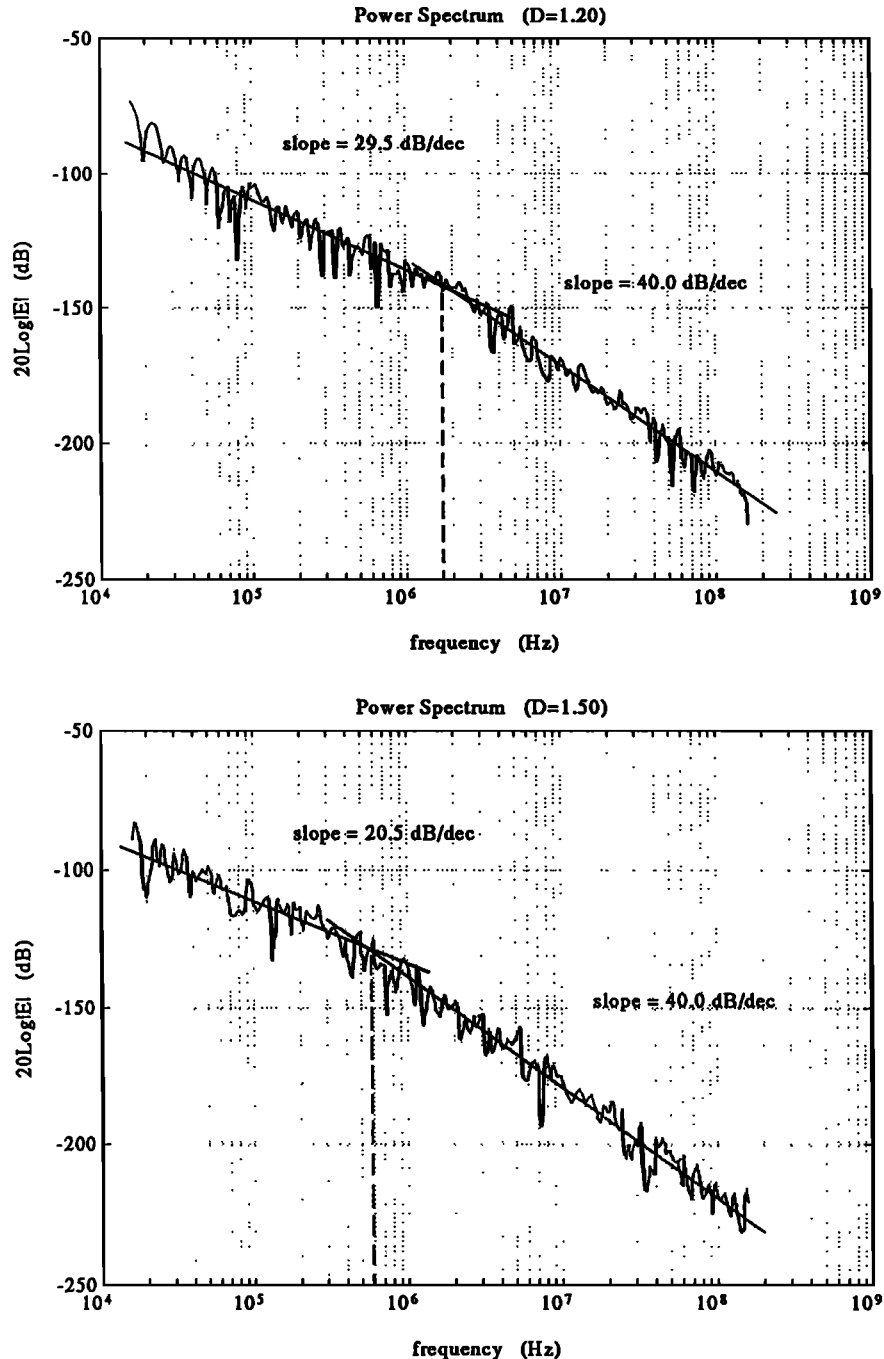


**Figure 4.** Evaluation of the fractal dimension: box counting (Strahle version). Graphical analysis of box counting associated with (a) the same channel and (b) the transient field as in Figure 2. In order to evaluate the fractal dimension (see text, section 2.2) data to be analyzed are normalized as follows: (a) with respect to the height of the channel (6000 m) and (b) with respect to the transient duration of the radiated field ( $300 \mu\text{s}$ ) for the horizontal axis and to the peak-to-peak field amplitude (1 V/m) for the vertical axis. The quantity  $2^m$  appearing on the horizontal axis is the reciprocal of the box size ( $= 1/2^m$ ) at step  $m$ , while the vertical axis is  $\log N_b(m)$ , as defined in section 2.2. The change of slope of the data corresponds to (a) about 90 m and (b) about  $0.9 \mu\text{s}$ .

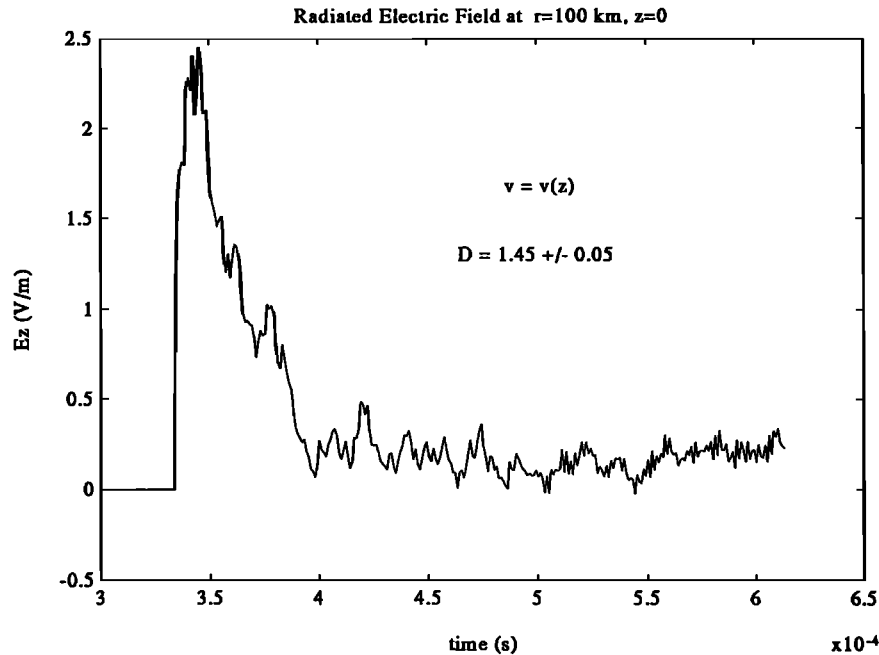


**Figure 5.** Spectral estimation of  $D_f$ . Power spectra of the fields radiated from the fractal channels of Figures 1 and 2. The low-frequency part of the spectrum is omitted. The slope of the envelope of the spectrum is (a)  $-29.5 \pm 0.5$  dB/decade and (b)  $-20.5 \pm 0.6$  dB/decade. The slope change of the envelope of the spectrum (see text) takes place (a) at about  $f_T = 1.6$  MHz and (b) at about  $f_T = 0.6$  MHz.

parent in the spectral fractal analysis as well. The results in Figure 5 show that in the high-frequency limit, all the spectra of the radiated field (for every value of the fractal dimension  $D_c$  of the channel) become parallel and decrease as  $1/f^4$ , corresponding to  $D = 1$ . In Figure 5, one can see that for frequencies beyond a threshold value (of about 1.6 MHz for the channel with  $D_c = 1.20$  and 0.6 MHz for the channel with  $D_c = 1.50$ ) the slope of the spectral envelope changes, decreasing as  $1/f^4$ ; again,  $\beta = 4$  corresponds to a  $D_c = 1$ .

This behavior is the counterpart of the time domain considerations. Namely, if the channel is fractal only for a spatial scale greater than  $\bar{L}$  ( $\bar{L} \approx 34$  m, for the case of  $D_c = 1.20$  and  $\bar{L} \approx 90$  m, for the case of  $D_c = 1.50$ ), resulting in a timescale,  $\bar{\tau}$  ( $\bar{\tau} \approx 0.34 \mu\text{s}$  and  $\bar{\tau} \approx 0.9 \mu\text{s}$  respectively), on the basis of standard signal analysis (sampling theorem, see [Papoulis, 1977, chap. 5]), we expect that for frequencies larger than a threshold value  $f_T = 1/2\bar{\tau}$  ( $f_T \approx 1.5$  MHz and

$f_T \approx 0.6$  MHz respectively) the channel behaves as a straight one (with  $D_c = 1$ ) and the spectral exponent accordingly tends to  $\beta = 4$ . This is actually observed in Figure 5.

### 3.3. Model Limitations

In this model, we have not considered propagation losses along the channel. The loss model present in the literature [Nucci *et al.*, 1990] amounts to a frequency-independent damping constant (as mentioned in section 2.1), and it can be seen (by carrying out the integral in (1)) that it does not alter the high-frequency part of the spectrum. The most relevant effect of loss correction is the elimination of the undamped pulse arising from the upper end of the channel, a feature that does not affect the analysis carried out here. Instead, channel losses shorten the duration of the radiated pulse: this latter effect might complement the present considerations. In fact, we have observed (see section 2.2) that the number  $m$  of iterations in the generation of

the channel sets the number  $N = 2^m$  of segments and the overall length  $L_{\text{tot}}$  of the channel, that is found to follow the law  $L_{\text{tot}} \propto 2^{m(D_c-1)}$  (the overall length has to be intended in an average sense, since path generation is random-based). The total duration of the transient radiated field is proportional to  $L_{\text{tot}}$  (see (4), (5), and (6)) and thus an exact fractal channel (i.e., an infinitely detailed one generated by  $m \rightarrow \infty$ ) would generate an unphysically persistent transient radiation in absence of losses. It is to be noted that a similar damping effect is attained here by the variable-velocity correction, since the pulse speed  $v$  enters the amplitude coefficients  $C_{\alpha,i}$  in (6). On the other hand, although fractal dynamics extends down to microscopical scales (not considered here explicitly), the assumptions employed here on the channel radiation, and therefore the considerations about tortuosity, cease to be meaningful below a certain spatial scale.

Last, in this work we have not considered the problem of noise on field data, which is instead typically added by any practical measurement, and which might alter the fractal properties of the field. Although this is a complex problem, for reasons of consistency we wish to address the issue here, without any claim of completeness. The noise does appear to be a special fractal [Peitgen and Saupe, 1988, chap. 2], and were its fractal dimension close to that of the phenomena under investigation, its effect would be difficult to separate from it. However, in that case the fractal dimension would not, of course, be significantly altered, and possible problems might arise only in the determination of the scales of fractality. Usually, the fractal dimension of noise, which equals 2 in the case of white noise [Peitgen and Saupe, 1988, chap. 2], appears to lie in the range 1.5–2.0 and is significantly higher than that of most observable channels, which rarely extends beyond 1.5 (the latter value is the dimension of a Brownian trail). In these cases, the problem of separation of noise from other fractal properties arises. In most cases, the separation can be made on the basis of the scales of fractality. More generally, the technique of

“fractal filtering” [Strahle, 1991], based on local fractal dimensions, can be employed to this aim.

#### 4. Summary and Conclusions

In this paper we have investigated the fractality hypothesis on the field generated by a discharge. Although we have confined ourselves to the case of a lightning discharge, the analysis should apply directly to in-air ESD (while in dielectrics field computation is complicated by air-dielectric inhomogeneity). Specifically, we have considered the radiation from a return stroke pulse traveling along a fractally tortuous channel. Within the framework of the simplifying assumptions (nondissipative channel, perfectly conducting ground), results demonstrate that the radiated field is a fractal and has the same fractal dimension as the channel within the confidence margins of the dimension-estimating algorithms. This suggests that the fractal dimension of the channel, that is, its tortuosity, can be given a measure, and especially, that this information on the channel can be inferred from the measured field data. These results lend some substance to the fractal modeling of the (fine structure) of the discharge radiation and indicate the importance of a fractal analysis of measured field data. First, one can think of making statistics of the fractal dimension of measured data, to be subsequently used in modeling. In fact, besides the importance of establishing the link between the fractal description of the source (discharge path) and of the field, this work serves also as a first step toward the development of a fractal model of discharges based on measured field data. In dealing with a tortuous channel, we have employed the same modeling assumptions that were present in previous works about this subject. At present, the authors are engaged in improving these models. From the more theoretical point of view, research is needed to prove (mathematically) the numerical evidence about the fractality and the dimension of the radiated field. Work in this direction, with extension to ESD, is presently in progress.

**Acknowledgments.** This work was supported in part by the EEC Science Project under grant SC1\*CT91-0690. The authors are glad to acknowledge several remarks by the reviewers that helped improve the quality of the paper.

## References

- Barnsley, M., *Fractals Everywhere*, 396 pp., Academic, San Diego, Calif., 1988.
- Baum, C. E., Return-stroke initiation, in *Lightning Electromagnetics*, edited by R. L. Gardner, pp.101-114, Hemisphere, New York, 1990.
- Baum, C. E., and L. Baker, Analytic return-stroke transmission-line model, in *Lightning Electromagnetics* edited by R. L. Gardner, pp.17-40, Hemisphere, New York, 1990.
- Boxleitner, W., *Electrostatic Discharges and Electronic Equipments*, 118 pp., IEEE Press, New York, 1989.
- Dubuc, B., J. F. Quiniou, C. Roques-Carmes, C. Tricot, and S. W. Zucker, Evaluating the fractal dimension of profiles, *Phys. Rev. A Gen. Phys.* 39 (3), 1500-1512, 1989.
- Fang, L., and W. Wenbing, An analysis of the transient fields of linear antennas, *IEEE Trans. Electromagn. Compat.*, 31 (4), 404-409, 1989.
- Felsen, L. B., and N. Marcuvitz, *Radiation and Scattering of Waves*, 888 pp., Prentice-Hall, Engelwood Cliffs N. J., 1973.
- Femia, N., L. Niemeyer, and V. Tucci, Fractal characteristics of electrical discharges: experiments and simulations, *J. Phys. D: Appl. Phys.*, 26, 619-627, 1993.
- Gagnepain, J. J., J. Gros Lambert, and R. Brendel, The fractal dimension of phase and frequency noises: Another approach to oscillator characterization, in *Proceedings of the 39th Annual Frequency Control Symposium* pp. 113-118, IEEE, New York, 1985.
- Gardner, R. L. (Ed.), *Lightning Electromagnetics*, 540 pp., Hemisphere, New York, 1990a.
- Gardner, R. L., Effect of the propagation path on lightning-induced transient fields, in *Lightning Electromagnetics*, edited by R. L. Gardner, pp. 139-153, Hemisphere, New York, 1990b.
- Jaggard, D. L., On fractal electrodynamics, in *Recent Advances in Eletromagnetic Theory*, edited by H. N. Kritikos and D. L. Jaggard, pp. 183-224, Springer-Verlag, New York, 1990.
- LeVine, D. M., and R. Meneghini, Simulation of radiation from lighting return strokes: The effect of tortuosity, *Radio Sci.*, 13 (5), 801-809, 1978a.
- LeVine, D. M., and R. Meneghini, Electromagnetic fields radiated from a lightning return stroke: Application of an exact solution to Maxwell's equations, *J. Geophys. Res.*, 83, 2377-2384, 1978b.
- Mandelbrot, B., *The Fractal Geometry of Nature*, 468 pp., W. H. Freeman, San Francisco, Calif., 1982.
- Nucci, C.A., G. Diendorfer, M.A. Uman, F. Rachidi, M. Ianoz, and C. Mazzetti, Lightning return stroke current models with specified channel-base current: A review and comparison, *J. Geophys. Res.*, 95, 20,395-20,408, 1990.
- Papoulis, A., *Signal Analysis*, 431 pp., McGraw Hill, New York, 1977.
- Paul, C. R., *Introduction to Electromagnetic Compatibility*, 765 pp., John Wiley, New York, 1992.
- Peitgen, H. O., and D. Saupe, *The Science of Fractal Images*, 312 pp., Springer-Verlag, New York, 1988.
- Strahle, W. C., Turbulent combustion data analysis using fractals, *AIAA J.*, 29, (3), 409-417, 1991.
- Tai, C. T., *Dyadic Green's Functions in Electromagnetic Theory*, 246 pp., Intext Educational Publishers, San Francisco, Calif., 1971.
- Uman, M. A., *The Lightning Discharge*, 377 pp., Academic, San Diego, Calif., 1987.

---

F. Canavero, D. Labate, and G. Vecchi, Dipartimento di Elettronica, Politecnico di Torino, Corso Duca degli Abruzzi, 24, I-10129 Torino, Italy.

(Received February 25, 1993; revised August 18, 1993; accepted October 18, 1993.)